Model calculations for the current-voltage characteristics of moving two-dimensional pancake vortex lattices in a finite stack of magnetically coupled superconducting thin films with transport current in the top layer

Thomas Pe, Maamar Benkraouda, and John R. Clem
Ames Laboratory, U.S. Department of Energy and Department of Physics and Astronomy, Iowa State University, Ames, Iowa 50011
(Received 14 April 1997)

We consider two-dimensional (2D) pancake vortices in a stack of N Josephson-decoupled superconducting films in an applied magnetic induction perpendicular to the layers and transport current applied to the top layer. We assume that the pancake vortices in every layer form lattices that have the same structure and are not rotated relative to each other, though we do not require them to be in perfect registry with one another. Current-voltage characteristics are calculated, corresponding to voltage-measuring circuits attached to the top and bottom layers. The effects of both zero and nonzero uniform pinning are investigated. For small currents, the pancake lattices either remain pinned or move with the same fixed velocity. But when the surface current density in the top layer exceeds a certain value, the calculated top and bottom voltages become different from each other. We then investigate the dependence of this decoupling surface current density on the applied magnetic induction, the pinning strength, and the number of layers. [S0163-1829(97)00438-4]

I. INTRODUCTION

The layered structure of the high-T_c cuprates has raised interesting questions as to the nature and properties of the vortices observed in these materials in the mixed phase. Detailed studies[1–5] starting from the well-known model of Lawrence and Doniach[6–9] have suggested that vortices in these layered superconductors may be thought of in terms of intralayer two-dimensional (2D) pancake vortices connected by interlayer Josephson strings. A simpler but very useful approach has also been considered in the literature,[1,2,10,4,11] whereby the weak interlayer Josephson coupling is neglected and the layered superconductor is treated as a stack of parallel thin films with pancake vortices in different layers interacting solely via magnetic coupling. This model has been applied to a wide variety of subjects, such as studies of vortex-lattice melting at low fields,[12,13] attractive long-range vortex-vortex interaction,[14] vortex interaction with defects,[15] and surface effects.[16]

In a recent paper,[17] we presented a detailed study of the magnetic coupling between 2D pancake vortices in a stack of N superconducting thin films, where the full discreteness of the layered structure was taken into account but no thermal fluctuation effects were incorporated. Our present aim is to extend that approach to the study of the dynamics of pancake vortices in a finite stack of Josephson-decoupled layers with a magnetic field applied perpendicular to the layers and with transport current injected in only one of the two outermost layers.

When there is no Josephson coupling between the superconducting layers, transport current injected into, say, the top layer remains confined to that layer, and only the top pancake vortices feel a Lorentz force associated with the applied current. The Lorentz force will tend to move the top pancake vortices, and this motion will then be opposed by the forces associated with viscous drag, pinning, and the magnetic coupling between the top pancake vortices and those in the lower superconducting layers. Likewise, a pancake in any of the lower layers will move if the net magnetic interaction force acting on it balances, if not exceeds, the opposing intralayer viscous drag and pinning forces.

In type-II superconductors, vortex motion leads to the appearance of a flux-flow voltage.[18] For the high-T_c materials, this voltage arising from the motion of vortices along the ab plane can be directly measured by attaching properly configured voltage-measuring circuits to the outermost layers. A theory for two magnetically coupled superconducting layers of finite thickness had been developed[19] and the corresponding current-voltage characteristics had been calculated.[20] These model calculations were made under the simplifying assumption that pinning in the layers was uniform; nevertheless, they were found to be in excellent agreement with the results of early flux-transformer experiments.[21,22] This close agreement has motivated us to consider in our present calculations not only the case of zero pinning, but also that of nonzero uniform pinning in $N \geqslant 2$ magnetically coupled thin films. Numerous experiments on the correlation of vortex motion in the high-T_c superconductors have already been done.[23–29] Within the limitations of our proposed model, we shall attempt in this paper to understand certain aspects of 2D pancake vortex dynamics in a stack of Josephson-decoupled layers that are relevant to current experimental investigations.

II. FORCE-BALANCED EQUATIONS

We consider a stack of N Josephson-decoupled superconducting thin films with interlayer spacing s and assume that the thickness d of each superconducting film is much less than each film's bulk penetration depth λ_s. The effective penetration depth for the decay of fields induced by currents flowing parallel to the layers is defined[30] via $\lambda_\parallel^2 = (s/d)\lambda_s^2$. The 2D screening length Λ can then be written[4] as either $2\lambda_\parallel^2/s$ or $2\lambda_s^2/d$, with some papers in the literature omitting the factor of 2.

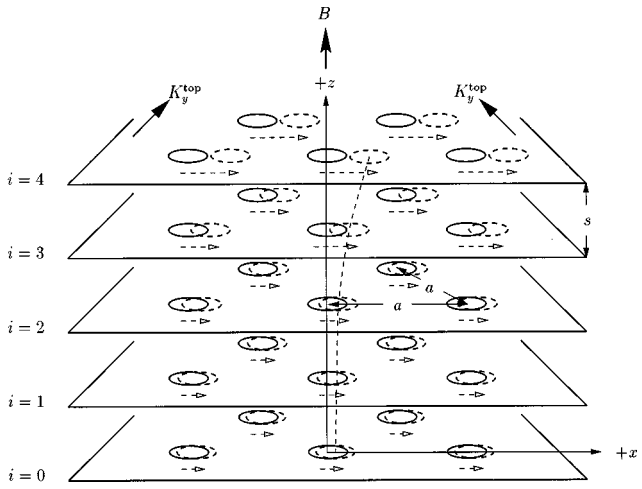

FIG. 1. A stack of five Josephson-decoupled superconducting layers with a surface current density K_y^{top} flowing in the top layer and a magnetic field B applied perpendicular to the layers. Each layer contains a perfect triangular 2D pancake vortex lattice with nearest-neighbor distance a. The pancakes drawn in solid lines correspond to when $K_y^{top}=0$, so that the lattices are in perfect registry. Under the influence of K_y^{top} and the interlayer magnetic coupling between pancakes, the lattices move away from their equilibrium positions. Such a situation is illustrated by the pancake lattices drawn in dashed lines.

We neglect the effects of thermal fluctuations and assume that, if we apply a magnetic induction B perpendicular to the layers, perfect 2D triangular lattices of pancake vortices form in the superconducting layers, as sketched in Fig. 1. Let a denote the nearest-neighbor distance between pancakes in each layer. At equilibrium with the applied field, the 2D pancake lattices are all in perfect registry. We choose the z axis to coincide with a vertical stack of 2D pancake vortices, such that the bottom layer is at $z=0$ while the top layer lies at $z=(N-1)s$. Moreover, we choose the x axis to lie along a nearest-neighbor direction of the pancake lattices. The 2D real lattice vectors in each layer can be written as[20]

$$\mathbf{l}=a[\hat{x}(l_1+l_2/2)+\hat{y}\sqrt{3}l_2/2\,], \tag{1}$$

where $\hat{x}$ and $\hat{y}$ are the unit vectors along x and y, and l_1 and l_2 take on all integer values. The corresponding reciprocal lattice vectors are[20]

$$\mathbf{g}=(2\pi/a)[\hat{x}g_1+\hat{y}(2g_2-g_1)/\sqrt{3}], \tag{2}$$

with g_1 and g_2 spanning all integers.

Now, suppose that we apply a constant surface current density $\hat{y}K_y^{top}$ to the top layer at time $t=0$ and neglect vortex pinning. Because of the combined action of K_y^{top} and the interlayer magnetic coupling, the 2D pancake lattices in the different layers will move in the x direction, away from their equilibrium positions. (Refer to Fig. 1 for the case of five superconducting layers.) Let $x_i(t)$ denote the displacement from equilibrium of the pancake lattice in layer i at time t. When $t=0$, $x_i(0)=0$ in all layers, $0\leqslant i\leqslant N-1$.

The balance of forces for a vortex in the 2D pancake lattice in layer i for $t>0$ is given by the following equation:

$$\eta\,\dot{x}_i=\sum_{j\neq i}F_{cx}(x_j-x_i,j,i)+\frac{\phi_o}{c}K_y^{top}\delta_{i,N-1}, \tag{3}$$

where η is the viscous drag coefficient, $\dot{x}_i$ is the time derivative of x_i, ϕ_o is the flux quantum $hc/2e$, and $\delta_{i,N-1}$ is a Kronecker δ. We assume overdamped vortex dynamics, so that we can neglect the term in the equation of motion involving the 2D pancake vortex inertial mass. The summation symbol $\Sigma_{j\neq i}$ means that i is excluded from a sum over j from 0 to $N-1$. F_{cx} is the x component of the magnetic coupling force exerted by the 2D pancake lattice in layer j on any pancake belonging to the lattice in layer i.

We can write F_{cx} in the following form:[17]

$$F_{cx}(x_j-x_i,j,i)=\frac{2}{\sqrt{3}\pi}\left(\frac{\phi_o}{\Lambda a}\right)^2\sum_{\mathbf{g}\neq\mathbf{0}}\frac{g_x}{g}C(g,j,i)\times\sin[g_x(x_j-x_i)]; \tag{4}$$

g and g_x denote the magnitude and the x component of $\mathbf{g}$, respectively, and

$$C(q,j,i)=\frac{\sinh qs\;Z(q,i,j)}{g(q)-h(q,N-1-j)-h(q,j)}. \tag{5}$$

The function g in the above expression is given by

$$g(q)=2[(1/q\Lambda)\sinh qs+\cosh qs]. \tag{6}$$

We define a function f:

$$f(q)=(1+2/q\Lambda)\sinh qs+\cosh qs. \tag{7}$$

As in Ref. 17, the functions h and Z that appear in Eq. (5) can be constructed using f and g:

$$h(q,n\geqslant 0)=\begin{cases}e^{-qs}, & n=0\\ 1/f(q), & n=1\\ 1/[g(q)-h(q,n-1)], & n>1,\end{cases} \tag{8}$$

$$Z(q,n,m)=\begin{cases}\displaystyle\prod_{p=0}^{m-n-1}h(q,m-p), & 0\leqslant n\leqslant m-1\\ 1, & n=m\\ \displaystyle\prod_{p=0}^{n-m-1}h(q,N-1-m-p), & m+1\leqslant n\leqslant N-1.\end{cases} \tag{9}$$

In the presence of uniform pinning of the pancake vortices in all the superconducting layers, Eq. (3) is replaced by

$$\eta\,\dot{x}_i=\sum_{j\neq i}F_{cx}(x_j-x_i,j,i)+\frac{\phi_o}{c}K_y^{top}\delta_{i,N-1}+F_{p\,i}. \tag{10}$$

Let K_c denote the magnitude of the critical depinning sheet current density in any of the superconducting layers. Whenever the sum of the first two terms on the right-hand side of Eq. (10) is greater than the maximum magnitude of the pinning force on a pancake vortex $\phi_o K_c/c$ we have $F_{p\,i}=-\phi_o K_c/c$, and when this sum is less than $-\phi_o K_c/c$, we have $F_{p\,i}=+\phi_o K_c/c$. However, when the magnitude of the sum of the first two terms on the right-hand side is less

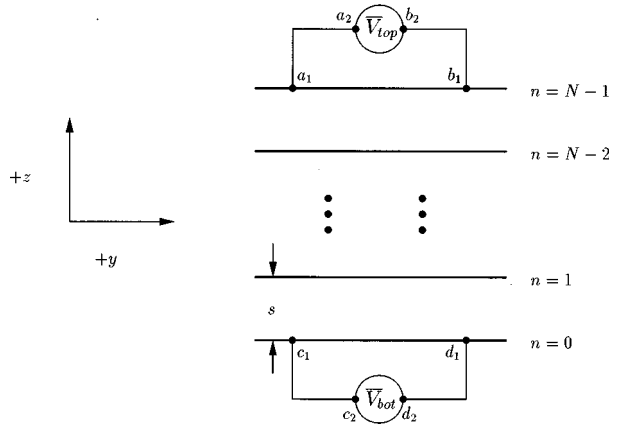

FIG. 2. Two voltage-measuring circuits in a layered superconductor, modeled as a stack of Josephson-decoupled superconducting layers. Each circuit consists of a high-impedance voltmeter connected by low-resistance leads to contact points on the sample. The leads of one circuit connect voltmeter terminals a_2 and b_2 to points a_1 and b_1 on the top layer. The other circuit has contacts c_1 and d_1 on the bottom layer connected to terminals c_2 and d_2. For simplicity, the line segments $\overline{a_1 b_1}$ and $\overline{c_1 d_1}$ are chosen to be parallel to the y axis. The measured time-averaged voltages per unit length along the top and bottom layers are $\overline{V}_{top}$ and $\overline{V}_{bot}$, respectively.

than $\phi_o K_c/c$, the pinning force $F_{p\,i}$ exactly balances the other two terms, such that both sides of Eq. (10) are zero, and the vortices in layer i are immobilized.

The resulting set of N force-balanced equations (i.e., one equation for each layer) can be integrated numerically so as to yield the displacements from equilibrium of all the N pancake lattices at $t>0$. From these solutions, one can then calculate the corresponding lattice velocities. We discuss in the next section the relation between these velocities and the time-averaged voltages measured in dc flux transformer experiments.

III. FLUX-FLOW VOLTAGE

Suppose we attach two voltage-measuring circuits to the stack of superconducting thin films described above, with a transport current density $K_y^{\rm top}$ flowing in the top layer, and a magnetic field applied parallel to the films. Each of these circuits consists of low-resistance leads connecting the specimen to the terminals of a sensitive high-impedance voltmeter. Let the contacts a_1 and b_1 of one of these circuits be situated on the top layer, with corresponding voltmeter terminals a_2 and b_2. As for the other circuit, let its contact points c_1 and d_1 be on the bottom layer, connected to voltmeter terminals c_2 and d_2. (See Fig. 2.) For simplicity, we assume that the line segments $\overline{a_1 b_1}$ and $\overline{c_1 d_1}$ are parallel to the y axis. The equations relating the motion of vortices with the voltages that are measured by such circuits have been treated extensively in Ref. 18.

Let us define time-averaged voltages per unit distance between contacts, $\overline{V}_{\rm top}$ and $\overline{V}_{\rm bot}$ corresponding to the top and bottom voltage-measuring circuits. Two flux-flow regimes are possible, depending on the value of $K_y^{\rm top}$. For small $K_y^{\rm top}$ values and sufficiently low pinning, the 2D pancake lattices remain magnetically coupled to each other, so that the steady-state velocities of the pancake lattices are the same and constant in time. In this regime,

$$\overline{V}_{top}=\overline{V}_{bot}=\frac{\phi_o v_{xo}}{cA}, \tag{11}$$

where v_{xo} is the terminal velocity component of the 2D lattices and A is the area of a lattice unit cell.

Once $|K_y^{\rm top}|$ exceeds a certain decoupling surface current density of magnitude K_d, however, the vortices in the top layer periodically slip relative to the vortices in the other layers. Consequently, the steady-state dynamics of the 2D pancake lattices can no longer be described by a single constant velocity. Instead, one finds that the velocities of all the 2D lattices are periodic in time, with a common period T. This follows from our having assumed that each 2D pancake lattice moves as a whole, with the nearest-neighbor distance a unchanged in time. Moreover, we see from Eq. (4) that the coupling force between any two pancake lattices in the stack is periodic in the relative displacement between the lattices, with a period equal to a. One can show that in this regime

$$\overline{V}_{top}=\frac{\phi_o}{cA}\frac{[x_{N-1}(t+T)-x_{N-1}(t)]}{T}, \tag{12}$$

$$\overline{V}_{bot}=\frac{\phi_o}{cA}\frac{[x_0(t+T)-x_0(t)]}{T}. \tag{13}$$

We therefore can compute $\overline{V}_{top}$ and $\overline{V}_{bot}$ for different values of $K_y^{\rm top}$ and K_c from the numerical solutions to the force-balanced equations discussed in the previous section. However, an accurate determination of the value of the decoupling surface current density K_d is still in order. An effective method for solving for this decoupling current density is discussed in the next section.

IV. DECOUPLING SURFACE CURRENT DENSITY

We begin by taking the simple case when $K_c=0$. Prior to switching on the flow of transport current $K_y^{\rm top}$ in the top layer, the 2D pancake vortex lattices in the different layers are assumed to be in perfect registry. When a sufficiently small value of $K_y^{\rm top}$ is turned on at $t=0$, these 2D pancake lattices remain magnetically coupled, so that all of them eventually move with a constant velocity component $v_{xo}\neq 0$.

We assume that at $t=0$, all pancake lattice displacements x_i are zero. It is convenient to choose a coordinate frame where the displacements x_i are transformed into new displacements X_i, such that

$$x_i(t)=X_i(t)+v_{xo}\,t, \tag{14}$$

for $0\leqslant i\leqslant N-1$. We then refer back to Eq. (3). In terms of the displacements X_i, the force-balanced equations for the pancake lattices below the top layer have the form

$$\eta\,\dot{X}_i=-\eta v_{xo}+\sum_{j\neq i}F_{cx}(X_j-X_i,j,i), \tag{15}$$

where $0\leqslant i\leqslant N-2$. As for the top pancake lattice, we have

$$\eta\,\dot{X}_{N-1}=-\eta v_{xo}+\sum_{j\neq N-1}F_{cx}(X_j-X_{N-1},j,N-1)+\frac{\phi_o}{c}K_y^{\rm top}. \tag{16}$$

A number of conditions must then be imposed on Eqs. (15) and (16). First of all, we note that for any layer i, $\dot{X}_i\to 0$ as $t\to\infty$ because $\dot{x}_i$ goes to v_{xo}. This tells us that $\Sigma_{i=0}^{N-1}X_i$ must become constant in time. Second, $\Sigma_{i=0}^{N-1}\Sigma_{j\neq i}F_{cx}(X_j-X_i,j,i)$ must be zero by Newton's third law. By applying these conditions directly to Eqs. (15) and (16), we obtain the following useful relation:

$$\eta\,v_{xo}=\frac{1}{N}\frac{\phi_o}{c}K_y^{\rm top}, \tag{17}$$

which holds so long as $K_y^{\rm top}$ is not sufficient to magnetically decouple the 2D pancake vortices in the different layers. What Eq. (17) tells us is that the magnetic interactions create a balance of forces such that when all vortices move with a common velocity component v_{xo} in the absence of pinning, the Lorentz force $\phi_o K_y^{\rm top}/c$ on any pancake vortex in the top layer divides equally among the N superconducting layers in order to balance the viscous drag force $-\eta\,v_{xo}$ on a vortex in any layer.

Let us suppose that X_{N-1} is fixed at some value for all time, and that the remaining displacements $X_0,\ldots,X_{N-2}$ are allowed to evolve in time from some appropriate starting values to the values corresponding to a force-balanced configuration of vortices. If t_o denotes the starting time, we can, for instance, choose $X_i(t_o)=-X_{N-1}(t_o)/(N-1)$ for all i in the range $0\leqslant i\leqslant N-2$, having assumed that $\Sigma_{i=0}^{N-1}\dot{X}_i(t)=0$ when $t\geqslant t_o$.

Taking the above approach, it follows from Eqs. (15), (16), and (17) that

$$\eta\,\dot{X}_i=\sum_{j\neq i}F_{cx}(X_j-X_i,j,i)+\frac{1}{N-1}\times\sum_{j\neq N-1}F_{cx}(X_j-X_{N-1},j,N-1) \tag{18}$$

for $0\leqslant i\leqslant N-2$, and

$$K_y^{\rm top}=-\frac{c}{\phi_o}\frac{N}{N-1}\sum_{j\neq N-1}F_{cx}(X_j-X_{N-1},j,N-1). \tag{19}$$

The $N-1$ equations of the form given by Eq. (18) can be integrated numerically to arrive at solutions for $X_0,\ldots,X_{N-2}$ that correspond to a given value of X_{N-1}. These solutions can then be inserted into the sum over magnetic coupling forces on the right-hand side of Eq. (19) in order to determine the value of $K_y^{\rm top}$. In this sense, we can say that each value of X_{N-1} corresponds to exactly one value of $K_y^{\rm top}$.

As it turns out, the range of $|K_y^{\rm top}|$ values associated with all possible X_{N-1} has an upper bound K_d. This means that if we apply a surface current density $K_y^{\rm top}$ in the top layer that exceeds K_d, then the magnetic coupling forces exerted on a pancake vortex in the top layer by any arrangement $X_0,\ldots,X_{N-2}$ of pancake lattices in the lower layers that satisfy Eq. (18) will be insufficient to balance the Lorentz force term $\phi_o K_y^{\rm top}/c$. The pancake vortex lattice in the top layer is thus magnetically decoupled from the other pancake lattices when $K_y^{\rm top}>K_d$; for this reason, we designate K_d as the decoupling surface current density. With the aid of Eq. (19), we can write

$$K_d=\frac{c}{\phi_o}\frac{N}{N-1}\sum_{j\neq N-1}F_{cx}(|X_j'-X_{N-1}'|,j,N-1), \tag{20}$$

where the displacements $X_0',\ldots,X_{N-1}'$ satisfy the $N-1$ force-balanced equations of the form given by Eq. (18) as well as maximize the magnitude of the net magnetic coupling force on any 2D pancake vortex in the top layer.

Suppose we now include the effects of uniform pinning on the 2D pancake vortices in every superconducting layer. With Eq. (10) taking the place of Eq. (3) at the start of the above discussion, we see that the force-balanced equation for the pancake lattice in layer $i\neq N-1$ has the form

$$\eta\,\dot{X}_i=-\eta\,v_{xo}+\sum_{j\neq i}F_{cx}(X_j-X_i,j,i)+F_{p\,i}, \tag{21}$$

whereas the equation for the top layer is

$$\eta\,\dot{X}_{N-1}=-\eta\,v_{xo}+\sum_{j\neq N-1}F_{cx}(X_j-X_{N-1},j,N-1)+\frac{\phi_o}{c}K_y^{\rm top}+F_{p\,N-1}. \tag{22}$$

Let the conditions imposed on Eqs. (15) and (16) be also applied to Eqs. (21) and (22). Furthermore, let us add the extra condition that when $v_{xo}\neq 0$, the pinning force on a pancake vortex in any layer must equal $\mp\phi_o K_c/c$, with the convention that the upper sign corresponds to $K_y^{\rm top}>0$, and the lower one to $K_y^{\rm top}<0$. Thus, when all vortices move with the same constant nonzero velocity in the presence of uniform pinning, we have

$$\eta\,v_{xo}\pm\frac{\phi_o}{c}K_c=\frac{1}{N}\frac{\phi_o}{c}K_y^{\rm top}, \tag{23}$$

which indicates that the Lorentz force on any pancake vortex in the top layer divides equally among the N superconducting layers in order to balance the sum of the viscous drag and pinning forces on a vortex in any layer.

As before, we can adopt the approach of fixing X_{N-1} for all time and allowing $X_0,\ldots,X_{N-2}$ to evolve in time from some appropriate starting values to those of a force-balanced configuration of vortices. Treating Eqs. (21), (22), and (23) in the same manner as we did with Eqs. (15), (16), and (17), we obtain once again Eqs. (18) and (19), suffering no modifications even though uniform pinning has now been included. This should not surprise us once we realize that uniform pinning becomes irrelevant when the pancake vortices have been brought to a final state where all of them are depinned and move at constant nonzero velocity. Hence, whether or not we have uniform pinning present, we arrive at exactly the same value of K_d that is needed to destroy con-

stant nonzero motion in a system of pancake vortices by magnetically decoupling the top pancakes from the rest.

Equation (23) also tells us that when all pancake vortices move with the same nonzero velocity, $|K_y^{\rm top}|$ is always greater than K_c by an amount $Nc\eta\,|v_{xo}|/\phi_o$. In other words, a uniformly moving system of pancake vortices is possible only if $NK_c<|K_y^{\rm top}|<K_d$. Vortex motion is suppressed as $t\to\infty$ when the value of $|K_y^{\rm top}|$ falls between zero and some activation value. This activation value equals NK_c when $NK_c<K_d$, and is K_d if $K_d<NK_c$. For $K_d<|K_y^{\rm top}|$, the pancake vortices in the top layer are obviously decoupled from the vortices in the other layers by virtue of the definition of the decoupling surface current density K_d.

Let us consider the limiting case when $\dot{x}_i\to 0$ as $t\to\infty$ for every layer i and for all $|K_y^{\rm top}|$ values ranging from zero up to K_d. We refer once again to Eq. (10). The force-balanced equations for the pancake vortex lattices below the top layer are of the form

$$\eta\,\dot{x}_i=\sum_{j\neq i}F_{cx}(x_j-x_i,j,i)+F_{p\,i}, \tag{24}$$

with $0\leqslant i\leqslant N-2$. The equation for the top pancake lattice $(i=N-1)$ is

$$\eta\,\dot{x}_{N-1}=\sum_{j\neq N-1}F_{cx}(x_j-x_{N-1},j,N-1)+\frac{\phi_o}{c}K_y^{\rm top}+F_{p\,N-1}. \tag{25}$$

Let us now fix the value of x_{N-1} in time and allow the remaining displacements to evolve. We can therefore use Eqs. (24) to solve numerically for $x_0,\ldots,x_{N-2}$ corresponding to the assumed time-independent value of x_{N-1}. Having calculated in this way for the displacements, we can apply them to Eq. (25) and note that $\dot{x}_{N-1}$ is zero for values of $K_y^{\rm top}$ such that

$$-\frac{\phi_o}{c}K_c<\sum_{j\neq N-1}F_{cx}(x_j-x_{N-1},j,N-1)+\frac{\phi_o}{c}K_y^{\rm top}<+\frac{\phi_o}{c}K_c. \tag{26}$$

Using the above condition, we can write

$$K_d=K_c+\frac{c}{\phi_o}\sum_{j\neq N-1}F_{cx}(|x_j'-x_{N-1}'|,j,N-1), \tag{27}$$

such that $x_0',\ldots,x_{N-2}'$ satisfy the force-balanced equations that derive from Eq. (25) and maximize the magnitude of the net magnetic coupling force exerted on any pancake vortex in the top layer by all vortices in the other layers.

V. NUMERICAL CALCULATIONS

Let us choose values for the interlayer spacing s and the penetration depth $\Lambda_\parallel$ that are typical of the high-T_c superconductor $Bi_2Sr_2CaCu_2O_x$. Specifically, we set s and $\lambda_\parallel$ to 1.5×10^{-7} cm and 2.5×10^{-5} cm, respectively. These values give $\Lambda\approx 8.4\times10^{-3}$ cm, so that $c\phi_o/\Lambda^2\approx 30$ mA/cm. The latter quantity is a convenient unit for the different surface current densities under consideration.

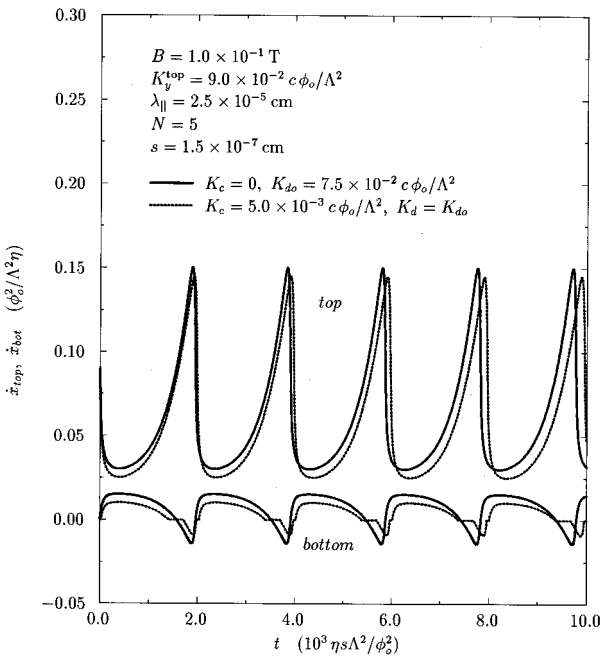

FIG. 3. Velocities $\dot{x}_{top}$ and $\dot{x}_{bot}$ of the top and bottom pancake vortex lattices as a function of time t for values of the critical surface current density K_c of a single layer equal to 0 and $5.0\times10^{-3}c\phi_o/\Lambda^2$. The number N of superconducting layers is 5 and the value of the magnetic induction B applied perpendicular to the layers is 1.0×10^{-1} T. For the high-T_c superconductor $Bi_2Sr_2CaCu_2O_x$, we can assume a penetration depth $\lambda_\parallel$ of 2.5×10^{-5} cm, and an interlayer spacing s of 1.5×10^{-7} cm. The applied surface current density $K_y^{\rm top}$ in the top layer is an input parameter set to $9.0\times10^{-2}c\phi_o/\Lambda^2$. Note that even for the nonzero K_c value considered, $K_d=K_{do}$, where K_d denotes the decoupling surface current density and K_{do} is the value of K_d in the absence of pinning (with a computed value of $7.5\times10^{-2}c\phi_o/\Lambda^2$ for the above parameter values). This is because the nonzero value of NK_c in this case remains less than K_{do}. Also note that $K_d<K_y^{\rm top}$ for the two cases of K_c considered. This is consistent with the nonconstant velocities obtained for the top and bottom pancake lattices. In these calculations, $K_y^{\rm top}$ is introduced instantaneously at $t=0$. Nevertheless, $\dot{x}_{top}$ and $\dot{x}_{bot}$ assume cyclic profiles within a few periods after the said current is introduced.

In Fig. 3, we show the characteristic time dependence of the top and bottom 2D pancake vortex lattice velocities $\dot{x}_{top}$ and $\dot{x}_{bot}$ in a stack of $N=5$ superconducting layers when the applied surface current density $K_y^{\rm top}$ in the top layer exceeds the decoupling surface current density K_d. The magnetic induction B directed perpendicular to the layers is assumed to be 1.0×10^{-1} T, whereas $K_y^{\rm top}$ is set to $9.0\times10^{-2}c\phi_o/\Lambda^2$. Although the full value of $K_y^{\rm top}$ is instantaneously introduced in the numerical calculations at the initial time $t=0$, both $\dot{x}_{top}$ and $\dot{x}_{bot}$ are practically periodic after an elapsed time interval of the order of the steady-state period.

Plots are given for values of the critical surface current density K_c of a single layer equal to 0 and $5.0\times10^{-3}c\phi_o/\Lambda^2$. Numerical calculations show that even though K_c is not zero in the latter case, the corresponding value of K_d is equal to that obtained in the former case that involves no pinning. This value, which we denote as K_{do}, is

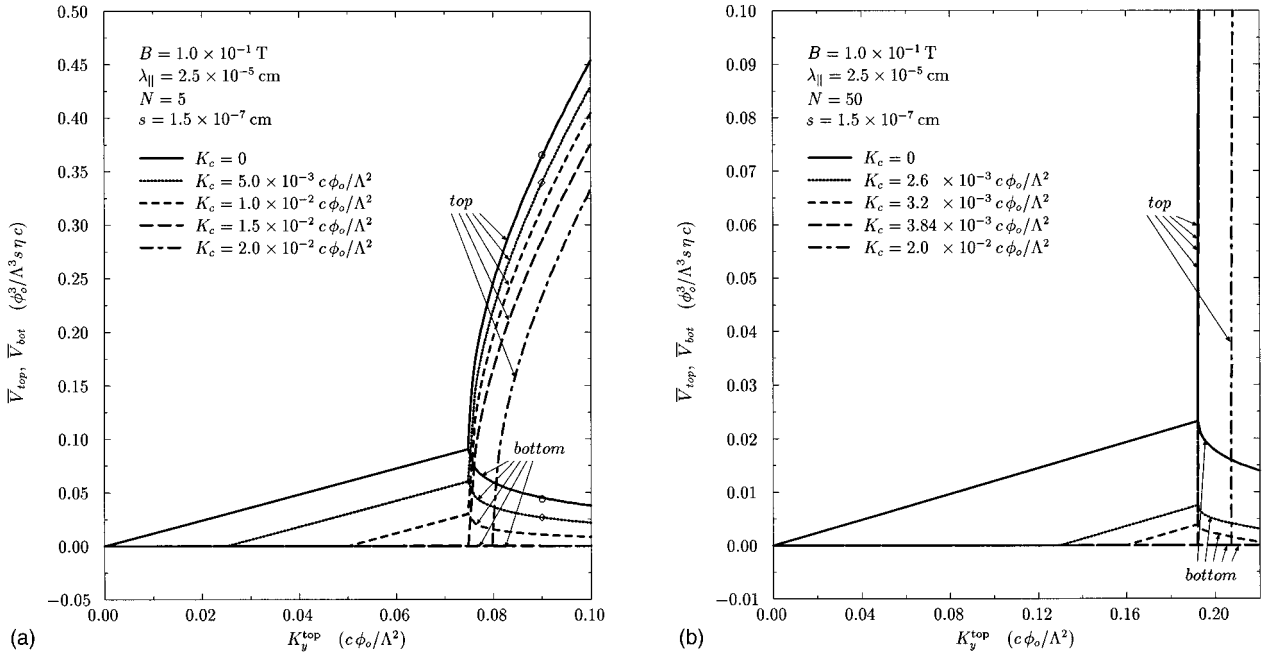

FIG. 4. (a) Time-averaged voltages per unit length, $\overline{V}_{top}$ and $\overline{V}_{bot}$, corresponding to the top and bottom voltage-measuring circuits in Fig. 2, shown as a function of the applied surface current density $K_y^{\rm top}$ at the top layer. We have assumed $N=5$ superconducting layers and a magnetic induction $B=1.0\times10^{-1}$ T applied perpendicular to the layers. The interlayer spacing s is assumed to be 1.5×10^{-7} cm, and the penetration depth $\lambda_\parallel$ is taken as 2.5×10^{-5} cm. Plots are given for values of the critical surface current density K_c of a single layer equal to 0, 5.0×10^{-3}, 1.0×10^{-2}, 1.5×10^{-2}, and $2.0\times10^{-2}c\phi_o/\Lambda^2$. In each case, the decoupling surface current density K_d can be identified as the value of K_y^{top} above which $\overline{V}_{top}$ and $\overline{V}_{bot}$ split into two distinct branches. The curves corresponding to the first four K_c values enumerated above have $0\leqslant NK_c\leqslant K_{do}$, where K_{do} is the decoupling surface current density in the absence of pinning. As in Fig. 3, K_{do} is calculated to be $7.5\times10^{-2}c\phi_o/\Lambda^2$. For the curves that correspond to the remaining value of K_c, we have $K_{do}<K_d<NK_c$, with K_d computed at $8.0\times10^{-2}c\phi_o/\Lambda^2$. The points marked by the symbols ○ and ◇ at $K_y^{top}=9.0\times10^{-2}c\phi_o/\Lambda^2$ give the values of $\overline{V}_{top}$ and $\overline{V}_{bot}$ for the two cases, $K_c=0$ and $5.0\times10^{-3}c\phi_o/\Lambda^2$, considered in Fig. 3. (b) Time-averaged voltages per unit length, $\overline{V}_{top}$ and $\overline{V}_{bot}$, corresponding to the top and bottom voltage-measuring circuits in Fig. 2, shown as a function of the applied surface current density K_y^{top} at the top layer. An applied magnetic induction $B=1.0\times10^{-1}$ T is directed perpendicular to $N=50$ superconducting layers. The interlayer spacing s is 1.5×10^{-7} cm, whereas the penetration depth $\lambda_\parallel$ is 2.5×10^{-5} cm. Curves are shown with values of the critical surface current density K_c of a single layer equal to 0, 2.6×10^{-3}, 3.2×10^{-3}, 3.84×10^{-3}, and $2.0\times10^{-2}c\phi_o/\Lambda^2$. The decoupling surface current density K_d is the value of K_y^{top} above which $\overline{V}_{top}$ and $\overline{V}_{bot}$ split into two distinct branches. For the curves with K_c equal to the first four values enumerated above, we have $0\leqslant NK_c\leqslant K_{do}$, where K_{do} is the decoupling surface current density in the absence of pinning. The calculated value of K_{do} in this figure is $1.92\times10^{-1}c\phi_o/\Lambda^2$. The curves having K_c equal to the remaining value fall within the region $K_{do}<K_d<NK_c$, with K_d equal to $2.07\times10^{-1}c\phi_o/\Lambda^2$.

approximately $7.48\times10^{-2}c\phi_o/\Lambda^2$. As discussed in the last section, the reason for this is that, although K_c is zero in one and nonzero in the other, the values of NK_c for both cases fall below the value of K_{do}.

The nonconstant, essentially periodic behavior of $\dot{x}_{top}$ and $\dot{x}_{bot}$ in time agrees with the conclusions drawn in the previous section for $NK_c<K_d<|K_y^{\rm top}|$. It is also clear from this figure that $\dot{x}_{top}$ (i.e., the pancake lattice velocity in the layer where all of the transport current flows) has a larger time-averaged value and a greater variance compared to $\dot{x}_{bot}$. The more complicated profile of the latter when $K_c=5.0\times10^{-3}c\phi_o/\Lambda^2$ is also worth noting. Aside from those regions where the bottom pancake lattice is immobilized by pinning, we also observe time intervals wherein the direction of lattice motion is reversed. This reversal, which can also be observed in the bottom curve corresponding to $K_c=0$, is entirely due to the assumption of perfect spatial periodicity for the pancake lattices at all times and to the attractive nature of the interaction between two such lattices belonging to different layers.

Figures 4(a) and 4(b) illustrate the K_c dependence of the time-averaged voltages per unit length, $\overline{V}_{top}$ and $\overline{V}_{bot}$, corresponding to the top and bottom voltage-measuring circuits shown in Fig. 2. Figure 4(a) assumes $N=5$ superconducting layers, whereas there are $N=50$ layers considered in Fig. 4(b). The applied magnetic induction B is set to 1.0×10^{-1} T in these two figures. Both of them also consider the special case when $K_c=0$, along with the following nonzero values of K_c: 5.0×10^{-3}, 1.0×10^{-2}, 1.5×10^{-2}, and $2.0\times10^{-2}c\phi_o/\Lambda^2$ for Fig. 4(a), and 2.6×10^{-3}, 3.2×10^{-3}, 3.84×10^{-3}, and $2.0\times10^{-2}c\phi_o/\Lambda^2$ for Fig. 4(b). As the plots clearly illustrate, $\overline{V}_{top}$ and $\overline{V}_{bot}$ are coincident when $K_y^{\rm top}$ is small, but break up into two distinct branches when $K_y^{\rm top}$ exceeds a certain value which is, by definition, K_d.

In both Fig. 4(a) and Fig. 4(b), we see that $0\leqslant NK_c\leqslant K_{do}$ for those curves corresponding to the four lowest values considered for K_c, so that the value of K_d remains equal to the pinning-free value K_{do}. However, the largest value of K_c considered in either figure has $K_{do}<NK_c$; in this case, K_d is

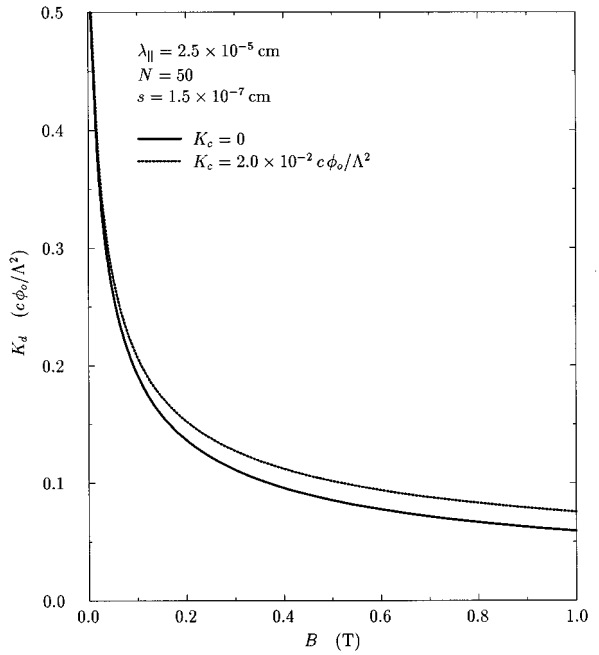

FIG. 5. The decoupling surface current density K_d as a function of the applied magnetic induction B directed perpendicular to $N=50$ superconducting layers. The penetration depth $\lambda_\parallel$ and the interlayer spacing s are 2.5×10^{-5} cm and 1.5×10^{-7} cm, respectively. The lower solid curve in this figure gives the B dependence of the pinning-free decoupling surface current density K_{do}. The upper dotted curve is for $K_c=2.0\times10^{-2}c\phi_o/\Lambda^2$, corresponding to the largest K_c value considered in Fig. 4(b).

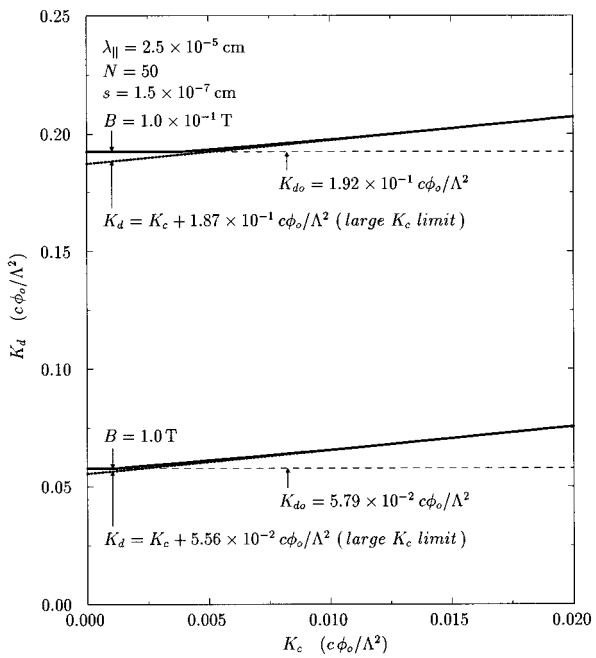

FIG. 6. The decoupling surface current density K_d plotted as a function of the critical surface current density K_c of a single layer. Plots are shown corresponding to values 1.0×10^{-1} T and 1.0 T for the applied magnetic induction B perpendicular to a stack of 50 superconducting layers. The interlayer spacing s is 1.5×10^{-7} cm whereas the penetration depth $\lambda_\parallel$ is 2.5×10^{-5} cm. K_{do} is the decoupling surface current density in the absence of pinning. The value of K_{do} is computed at 1.92×10^{-1} and $5.79\times10^{-2}c\phi_o/\Lambda^2$ for B equal to 1.0×10^{-1} T and 1.0 T, respectively. For $K_c\leqslant K_{do}/N$, we have $K_d=K_{do}$ (the horizontal dashed lines in the figure). But when $K_c>K_{do}/N$, K_d increases almost linearly with K_c. This linear behavior (shown in dotted lines) corresponding to the large K_c limit has the form $K_d=K_c+K_o$, where K_o is proportional to the coupling force on the top pancake lattice due to all the other pancake lattices rigidly fixed to their initial (i.e., zero transport current) positions. The computed values of K_o are $1.87\times10^{-1}c\phi_o/\Lambda^2$ for the smaller field and $5.56\times10^{-2}c\phi_o/\Lambda^2$ for the larger field.

greater than K_{do} and the time-averaged velocity of every pancake in the bottom layer is essentially zero for all values of K_y^{top}. In contrast to this, we note that so long as $NK_c<K_{do}$, the top and bottom pancakes move with the same average velocity, resulting in the same measured voltage in both the top and bottom circuits. This measured voltage is zero if $K_y^{top}<NK_c<K_{do}$, and is nonzero for $NK_c<K_y^{top}<K_{do}$. Finally, we see that whatever the relationship holds between the values of NK_c and K_{do}, the measured voltage increases in the top circuit and tends to zero in the bottom circuit as K_y^{top} is increased above the decoupling value K_d.

Figure 5 gives the B dependence of K_d for $K_c=0$ and $K_c=2.0\times10^{-2}c\phi_o/\Lambda^2$ in a stack of 50 superconducting layers. The curves show a monotonic decrease in the value of the decoupling surface current density with increasing B. For large values of the magnetic induction, this dependence goes as $1/\sqrt{B}$ to good approximation. This behavior is qualitatively the same as the field dependence of K_d discussed in Ref. 17 for a stack of pinning-free superconducting layers with equal but oppositely directed transport currents flowing in the top and bottom layers. In addition, we note that the two curves in this figure merge in the vicinity of zero magnetic induction, indicating that K_d does not seem to depend on the value of K_c in the weak-field limit.

Characteristic curves showing the dependence of K_d on K_c for 50 layers and for 1.0×10^{-1} T and 1.0 T fields are given in Fig. 6. In these curves, we observe that K_d remains equal to the pinning-free value K_{do} for nonzero values of K_c less than or equal to K_{do}/N. We also observe that beyond this value and onto the large K_c limit, the dependence of K_d on the critical surface current density is practically linear. This is easily understood as follows. We recall that the magnitude of the magnetic coupling force exerted by the pancakes in the top layer on a pancake in any of the lower layers has a finite maximum value. If the pinning force $\phi_o K_c/c$ is sufficiently large compared to this maximum, then the pancake in the lower layer is decoupled from the motion of pancakes in the top layer, undergoing little or no displacement from their equilibrium positions. In this case, therefore, the value of the sum over magnetic coupling forces on the right-hand side of Eq. (27) becomes independent of K_c, and the K_c dependence of K_d reduces to a simple linear dependence, having a slope equal to unity. This approach to linear behavior in the large K_c limit is clearly illustrated in Fig. 6.

Lastly, Fig. 7 shows the dependence of K_d on the quantity Ns for values of K_c equal to 0 and $5.0\times10^{-3}c\phi_o/\Lambda^2$, and for values of B equal to 1.0×10^{-1} and 1.0 T. As we have done in Fig. 5, we refer back to Ref. 17 and observe that the

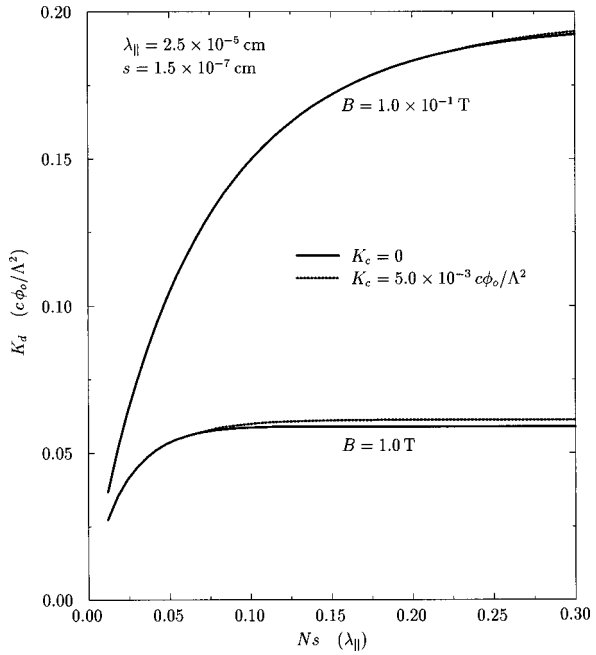

FIG. 7. The decoupling surface current density K_d plotted as a function of Ns. The values considered for the critical surface current density K_c are 0 and $5.0\times10^{-3}c\phi_o/\Lambda^2$. For each of these values, plots are shown corresponding to 1.0×10^{-1} T and 1.0 T for the applied magnetic induction B perpendicular to the superconducting layers. As is in the preceding plots, the interlayer spacing s is 1.5×10^{-7} cm and the penetration depth $\lambda_\parallel$ is 2.5×10^{-5} cm. Notice that for fixed B, the value of K_d in the large Ns limit is approached more gradually for $K_c\neq0$ than for $K_c=0$.

general features of the dependence of K_d on Ns in that paper are the same as in Fig. 7. In particular, the value of K_d approaches a saturation value as the number of layers considered is increased. For $K_c=0$, this saturation value is attained when Ns is of the order of the pancake vortex lattice spacing a. For a qualitative explanation of this feature, we refer the reader to the arguments presented in Ref. 17, which are also applicable to the present situation. As for the curves where K_c is nonzero, we observe that K_d also reaches its saturation value when Ns is $O(a)$, but this approach is attained more gradually with increasing Ns than in the approach where no pinning is present.

VI. SUMMARY

In this paper, we extended the approach that we had developed in Ref. 17 to the study of the dynamics of 2D pancake vortex lattices in a stack of N Josephson-decoupled layers with transport current flowing in the top layer. Both zero and nonzero uniform pinning in the superconducing layers were considered, but thermal fluctuations were not within the compass of our present investigations. The discussions and calculations involving nonzero uniform pinning were largely motivated by the success of previous studies[19,20] incorporating this feature in explaining very accurately the results of early flux transformer experiments done with two superconducting layers.[21,22]

Using our model, we considered voltage measuring circuits connected to the top and bottom layers and then calculated the corresponding theoretical current-voltage characteristics. The resulting plots showed that the pancakes in the top layer magnetically decouple from the pancakes in the other layers once a certain value K_d of the surface current density in the top layer is reached and exceeded. The dependence of this decoupling surface current density on the quantities B, K_c, and Ns were investigated. We showed that by increasing B, the value of K_d decreases monotonically, and that this dependence goes approximately as $1/\sqrt{B}$ for large values of B. We then demonstrated that in the large K_c limit, K_d increases linearly with K_c. Finally, we saw that the decoupling surface current density initially increases and then reaches a saturation value as Ns is increased. This saturation value is attained for $K_c=0$ and for $a<\lambda_\parallel$ when Ns is of the order of or greater than a, but this approach to saturation is moderated by the presence of nonzero uniform pinning.

ACKNOWLEDGMENTS

We thank V. G. Kogan and R. G. Mints for helpful discussions. Ames Laboratory is operated for the U.S. Department of Energy by Iowa State University under Contract No. W-7405-Eng-82.

[1] S. N. Artemenko and A. N. Kruglov, Phys. Lett. A **143**, 485 (1990).
[2] M. V. Feigel'man, V. B. Geshkenbein, and A. I. Larkin, Physica C **167**, 177 (1990).
[3] S. Chakravarty, B. I. Ivlev, and Yu. N. Ovchinnikov, Phys. Rev. B **42**, 2143 (1990).
[4] J. R. Clem, Phys. Rev. B **43**, 7837 (1991).
[5] L. N. Bulaevskii, M. Ledvij, and V. G. Kogan, Phys. Rev. B **46**, 366 (1992).
[6] W. E. Lawrence and S. Doniach, in *Proceedings of the 12th International Conference on Low Temperature Physics, Kyoto, 1970*, edited by E. Kanda (Keigaku, Tokyo, 1970), p. 361.
[7] L. N. Bulaevskii, Zh. Eksp. Teor. Fiz. **64**, 2241 (1973) [Sov. Phys. JETP **37**, 1143 (1973)].
[8] R. Klemm, M. R. Beasley, and A. Luther, J. Low Temp. Phys. **16**, 607 (1974).
[9] K. B. Efetov, Zh. Eksp. Teor. Fiz. **76**, 1781 (1977) [Sov. Phys. JETP **49**, 905 (1979)].
[10] A. Buzdin and D. Feinberg, J. Phys. (France) **51**, 1971 (1990).
[11] K. H. Fischer, Physica C **178**, 161 (1991).
[12] D. Fisher, M. P. A. Fisher, and D. Huse, Phys. Rev. B **43**, 130 (1991).
[13] G. Blatter, V. Geshkenbein, A. Larkin, and H. Nordborg, Phys. Rev. B **54**, 72 (1996).
[14] G. Blatter and V. Geshkenbein, Phys. Rev. Lett. **77**, 4958 (1996).
[15] A. Buzdin and D. Feinberg, Physica C **303-311**, 256 (1996).
[16] R. G. Mints, I. B. Snapiro, and E. H. Brandt, Phys. Rev. B **54**, 9458 (1996).

[17] T. Pe, M. Benkraouda, and J. R. Clem, Phys. Rev. B **55**, 6636 (1997).
[18] J. R. Clem, Phys. Rep. **75**, 1 (1981).
[19] J. R. Clem, Phys. Rev. B **12**, 1742 (1975).
[20] J. R. Clem, Phys. Rev. B **9**, 898 (1974).
[21] J. W. Ekin, B. Serin, and J. R. Clem, Phys. Rev. B **9**, 912 (1974).
[22] J. W. Ekin and J. R. Clem, Phys. Rev. B **12**, 1753 (1975).
[23] R. Busch, G. Ries, H. Werthner, G. Kreiselmeyer, and G. Saemann-Ischenko, Phys. Rev. Lett. **69**, 522 (1992).
[24] H. Safar, E. Rodríguez, F. de la Cruz, P. L. Gammel, L. F. Schneemeyer, and D. J. Bishop, Phys. Rev. B **46**, 14 238 (1992).
[25] Y. M. Wan, S. E. Hebboul, D. C. Harris, and J. C. Garland, Phys. Rev. Lett. **71**, 157 (1993).
[26] H. Safar, P. L. Gammel, D. A. Huse, S. N. Majumdar, L. F. Schneemeyer, D. J. Bishop, D. López, G. Nieva, and F. de la Cruz, Phys. Rev. Lett. **72**, 1272 (1994).
[27] D. López, E. Rodríguez, G. Nieva, F. de la Cruz, and S. W. Cheong, Physica B **194-196**, 1977 (1994).
[28] D. López, G. Nieva, and F. de la Cruz, Phys. Rev. B **50**, 7219 (1994).
[29] T. S. Lee, N. Missert, L. T. Sagdahl, J. Clarke, J. R. Clem, K. Char, J. N. Eckstein, D. K. Fork, L. Lombardo, A. Kapitulnik, L. F. Schneemeyer, J. V. Waszczak, and R. B. van Dover, Phys. Rev. Lett. **74**, 2796 (1995).
[30] J. R. Clem, Physica C **162-164**, 1137 (1989).